

# LIDAR INVESTIGATION OF AEROSOL PARTICLE SIZE DISTRIBUTION UNDER CUMULUS BASE

T. Stacewicz<sup>1</sup>, M. Posyniak<sup>2</sup>, S.P. Malinowski<sup>2</sup>, A.K. Jagodnicka<sup>1</sup>, S. Sitarek<sup>3</sup>, S. Arabas<sup>1</sup>

<sup>1</sup>Institute of Experimental Physics, Faculty of Physics, Warsaw University,  
ul. Hoża 69, 00-681 Warsaw, Poland

<sup>2</sup>Institute of Geophysics, Faculty of Physics, Warsaw University  
ul. Pasteura 7, 02-093 Warsaw, Poland

<sup>3</sup>Institute of Applied Optics, ul Kamionkowska 18. 03-805 Warsaw, Poland

## 1. INTRODUCTION

In the updraft, below the base of convective cloud the boundary layer aerosol becomes hydrated due to increase of relative humidity in adiabatic lift. Cloud Condensation Nuclei (CCN) are activated and small droplets are formed. In 1959 Twomey [1] elaborated model of this process that is still considered a valid one. The refined and improved versions of this approach are widely used for numerical modeling of convective processes, [2, 3] and to elucidate in-situ measurements [4]. There are, however, many uncertainties related with the details of droplet formation, particularly important in context of indirect aerosol influence on the radiative forcing [5]. Remote retrievals of vertical profiles of the aerosol size distribution can help in better understanding of the microphysical processes at the cloud base. Here we present a technique to investigate CCN activation and preliminary phase of droplet growth at base of convective cloud using multiwavelength lidar. It combines on a natural technique of aerosol particle size distribution (APSD) retrieval described in [6] and additional information on CCN activation from Twomey model [1].

Briefly the method consists in assumption of APSD function in a predefined form with several free parameters. In particular, for our three wavelength lidar we chose a bimodal combination of lognormal functions. The aerosol is assumed to consist of spheres of known refractive index. Such conditions are well fulfilled for the hygroscopic aerosol at high relative humidities close to the cloud base and for small cloud droplets. Using Mie approach [7] we calculate backscattering coefficient  $\beta_\lambda(z)$  and total scattering

coefficient  $\alpha_\lambda(z)$  for each wavelength  $\lambda$  in a range of distances  $z$  from the lidar located at  $z_0$ . After substitution of obtained parameters to a set of lidar equations :

$$L_\lambda(z) = A_\lambda \beta_\lambda(z) \exp \left[ -2 \int_{z_0}^z \alpha_\lambda(x) dx \right], \quad (1)$$

the range corrected calculated signals  $L_\lambda(z)$  are compared to the measured ones.

Direct substitution of extinction and backscattering coefficients into (1) ensures that APSD remains as the only unknown function in the system of equations. Application of the minimization procedure provides an opportunity to get the optimal parameters characterizing the predefined APSD distribution. The method does not require knowledge of lidar ratio.

## 2. LIDAR, EXPERIMENT AND SIGNALS REGISTERED UNDER CUMULUS CLOUD

Construction of the lidar used in observations of Cumulus base was described elsewhere [6, 8]. Briefly, in the optical transmitter pulsed Nd:YAG laser generates the beams at 1064, 532 and 355 nm. The energy of the light pulses reaches 100 mJ, the repetition rate is 10 Hz. In the optical receiver a Newtonian telescope with the mirror of 400 mm in diameter and focal length equal 1200 mm is used. The return light pulses, collected by the telescope, are spectrally separated by a polychromator and registered in relevant channels, corresponding to consecutive wavelengths. The signals from the photomultipliers installed at each channel are digitized by 12-bit A/D converters.

Lidar data analyzed in this study were

collected in Warsaw on 30. 08. 2008. On this day fair weather cumuli were developing in a mass of marine polar air advecting from north in peripheries of the Scandinavian high pressure system. The laser beams were sent vertically, pointing at clouds drifting above the lidar station. Cloud base height was increasing in course of measurements. Moreover, wind shear caused that clouds were tilted and signature of clouds in lidar profiles was observed at altitudes in a range from 1400 to 2000 m.

Fig.1 presents an example of range-corrected lidar profiles from the region classified as a cloud base. These profiles were obtained by averaging over 300 laser shots (30 s) and over 9 m long segments along the beam.

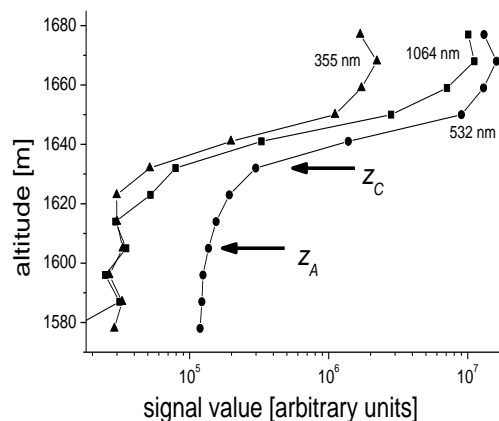


**Fig. 1.** Example of range corrected lidar signals in vicinity of the cumulus cloud base.  $z_A$  and  $z_C$  denote the activation and the condensation altitudes respectively

In general, presented profiles are typical for the lidar signals at the cloud base, as reported e.g. in [9] and [10]. At the altitudes below 1.6 km (i. e. more than 40 m below the cloud base) the signals are weak, which indicates that the light is scattered by aerosol consisting of small particles. For these altitudes the technique of retrieval, described in [6] was applied in its generic form. Beginning from 1605 m (the lower arrow in Fig. 1) all three signals increase. That indicates the enhanced scattering due to hygroscopic aerosol particle size growth. The corresponding height is denoted  $z_a$ , and is considered a signature of activation of CCN beginning. In this region we change the retrieval algorithm using additional

information, i.e. Twomey's model of CCN activation in adiabatic parcel. Its details are described in the next section.

Above the signal maximum (1670 m) lidar returns are strongly affected by multiple light scattering. Consequently, the signals above the maximum are not analyzed.

In course of measurements about 65 three wavelength profiles with cloud signature was collected. 12 of them was classified as pointing into the cloud base within the whole averaging period. For all 65 "cloudy" profiles a modified retrieval accounting for CCN activation and droplet growth was applied, but the statistical analysis of retrieval was performed separately for "cloud base" and "cloud side" cases, in order to look for differences. By principle the method should work for uniform cloud bases only.

### 3. PARCEL MODEL CALCULATIONS OF CCN ACTIVATION

Starting from the activation altitude,  $z_a$  (method of  $z_a$  determination is described in the next part) a simple model of CCN condensation and droplet growth, based on adiabatic parcel approach was used to provide additional information on vertical profiles of the particle distributions. Calculations of the evolution of CCN and droplet size distributions were performed with the accurate and efficient numerical code described in [11].

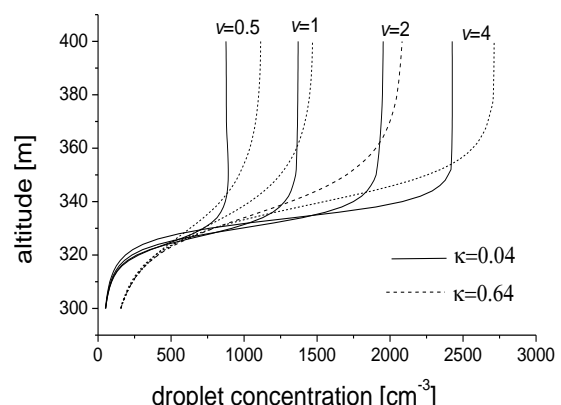


**Fig. 2.** Effective radius as a function of relative altitude for various lift speed  $v$  [m/s] and hygroscopicity coefficient  $\kappa$ .

Thermodynamic conditions were taken from the atmospheric sounding from 12 UTC from nearby (~25 km north) Legionowo (WMO

123740). Typical well mixed boundary layer was observed. Aerosol evolution in updraft was calculated using  $\kappa$ -Koehler approach [12]. Computations were done for constant updraft velocities at the cloud base ranging from 0.1 to 4.0 m/s and two values of  $\kappa$ : 0.04 (non-hygroscopic aerosol) and 0.64 (hygroscopic aerosol). Example results, shown in Fig. 2, indicate that to the first approximation number of the activated particles increases with the updraft velocity, while the depth of activation zone depends on the hygroscopicity of aerosol.

The initial modal distribution of aerosol retrieved from the lidar profile analysis below  $z_a$  was taken for the calculations. The starting level for all model runs was about 350 m below cloud base, and the simulations were stopped after reaching 500 m above the starting level. The following conclusions were drawn from the parcel model:

a) In the range of investigated updraft velocities and for hygroscopicity parameter from 0.04 (non-hygroscopic aerosol) to 0.64 (highly hygroscopic aerosol), the particles of dry radius which exceeds  $r_{min}=100\pm 20$  nm, are activated and grow into cloud droplets. Thus the droplet number concentration in cloud can be estimated from the integration of the right part of the APSD at the activation level  $z_a$  :

$$N_A = \int_{r_{min}}^{\infty} n(r) dr \quad (2)$$

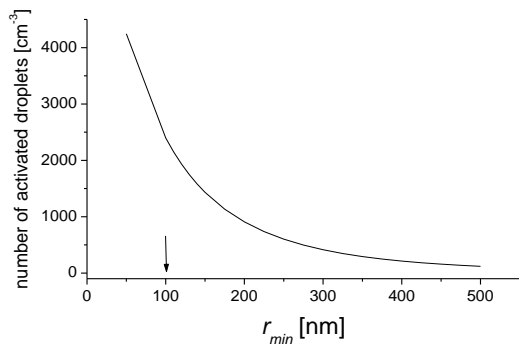


**Fig. 3.** Number of activated particles as a function of  $r_{min}$ . The arrow indicates  $r_{min}$  value.

The value of  $N_A$  as a function of  $r_{min}$  is presented in Fig. 3. While in this preliminary study the initial APSD is determined with precision of 50 % and the  $r_{min}$  with precision 20 %, the estimated droplet number

concentration in investigated clouds is  $N_A = 2400 \pm 1000$   $\text{cm}^{-3}$ , which is the value expected in polluted urban area.

b) Starting from the activation altitude  $z_A$  activated droplets constitute the Gaussian distribution. Its amplitude increases with height due to growing number of activated droplets. Median radius of the mode  $r_0$  and its width  $\sigma$  remains constant:  $r_0 \approx 1000$  nm,  $\sigma \approx 500$  nm

c) For the particles smaller than  $r_{min}$  the APSD remains unchanged.

d) At the altitude  $z_c$ , all hygroscopic particles of dry radii  $r > r_{min}$  become activated. Further growth (for  $z > z_c$ ) of activated droplets takes place due to the condensation. It can be expressed by increase of the median radius of Gauss mode with the constant amplitude.

#### 4. RETRIEVAL OF APSD IN UPDRAFT

Basing on the above conclusions a modified algorithm for retrieval of APSD in updraft under cumulus base consists of the following steps:

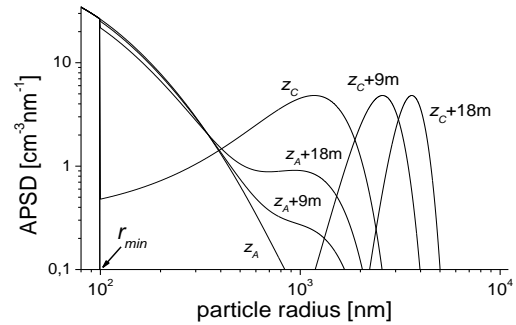


**Fig. 4.** Changes of Aerosol Particle Size Distribution with altitude, starting from activation altitude  $z_A$  for and consecutive altitudes to the condensation altitude  $z_C$  and above.

a) An initial guess of  $z_a$  altitude.

The first guess is an altitude above which a systematic increase of all three lidar signals is observed. At this level the APSD function, which was determined for  $z < z_a$ , is divided in two parts: for  $r < r_{min}$  it persists in its initial form while for  $r \geq r_{min}$  a Gaussian mode containing  $N_a$  particles is generated. Then the backscattering and total scattering coefficients ( $\beta_\lambda(z)$  and  $\alpha_\lambda(z)$ ) are calculated for each wavelength  $\lambda$  with Mie approach [7]. Using the formula (1) the range corrected

lidar signals  $L_\lambda(z)$  are found and compared to the measured ones. Fit provides the opportunity to determine the amplitude of the Gauss mode.

b) Since the determination of  $z_a$  is ambiguous, the procedure is repeated starting from the neighboring altitudes ( $z_A \pm 9$  m etc.). The smoothness of increase of the Gauss mode amplitude with the altitude is evaluated for each level.

After such iteration procedure the activation altitude is finally determined. The following evolution of the modeled aerosol particle size distribution within the activation range  $z_A < z < z_C$  are shown in Fig. 4.

c) Above the condensation altitude  $z_c$  the increase of the lidar signals (Fig. 1) result from the condensational growth of activated droplets, i.e. by the increasing median radius  $r_0$  at the constant number concentration  $N_A$ . Comparison of synthetic lidar signal calculated using this assumption to the measured one provides opportunity to determine  $r_0$  for each altitude.

Within these consecutive steps the size distribution function  $n(r, z)$  for each observed altitude can be determined (Fig. 4) and used e.g. to calculate the effective radius of droplets expressed by:

$$r_{eff}(z) = \frac{\int r^3 n(r, z) dr}{\int r^2 n(r, z) dr} \quad (3)$$

## 5. RESULTS AND DISCUSSION

Figs. 5 and 6 present statistics of lidar retrievals of activation/condensation at the cloud base. Due to the variability of cloud base heights their altitude was normalized to  $z_C$  for each lidar profile.

It can be seen, that the cases classified as “cloud base” are characterized with a smaller spread of activated droplets number and of the effective radius than the cases classified as “cloud side”. This confirms that usage of parcel model of droplet growth is useful in the retrieval procedure.

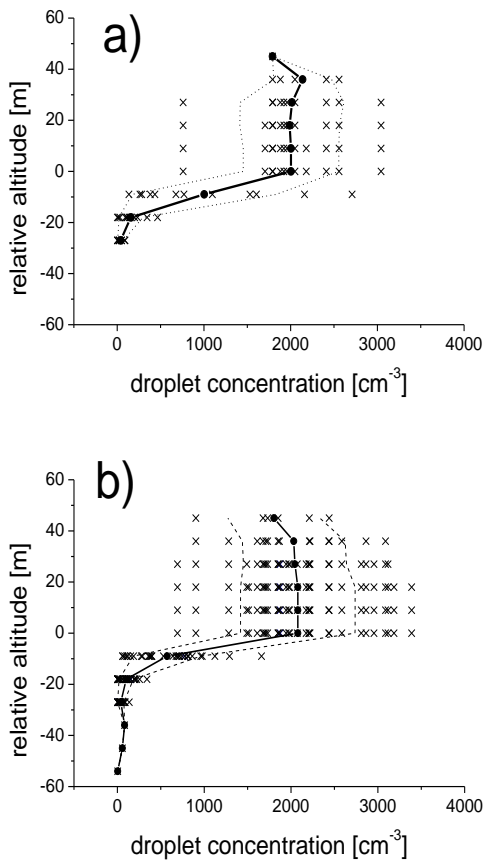


**Fig. 5.** Number of activated droplets as a function of the relative altitude ( $z_c=0$ ) retrieved for profiles classified as “cloud base” (a) and “cloud side” (b)

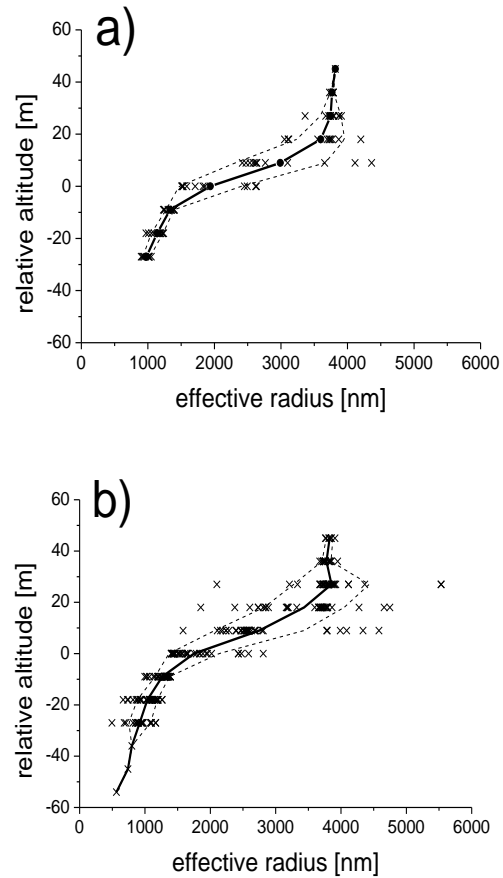


**Fig. 6.** Effective radius as a function of relative altitude ( $z_c=0$ ) in profiles classified as “cloud base” (a) and “cloud side” (b)

Decrease of  $N_A$  and fluctuations of  $r_{\text{eff}}$  at the topmost end of “cloud base” profiles are the effects of low-number statistics (only few shots reach this level). On the other hand similar effect is visible in the profiles classified as “cloud side”. This suggests the artifacts due to secondary scattering, which means that two topmost points should be rejected.

A sharp tilt in  $N_a$  at  $z=0$  and constant  $N_a$  above is the effect of retrieval assumptions, not of non-hygroscopic aerosol (c.f.  $N_a$  profiles from parcel model in Fig.2.). Comparison of Figs 2 and 5 suggests that the most probable updraft speed at the cloud base is  $\sim 2$  m/s.

In summary we may conclude that:

a) Information from parcel model of activation and condensational growth of cloud droplets can be used to estimate the cloud droplet number concentration  $N_a$  at the cloud base from multiwavelength lidar signals.

b) Additionally, the method allows estimating vertical profile of the effective radius of cloud droplets at the cloud base.

c) Comparison of measured lidar profiles at the cloud base to lidar profiles calculated theoretically with the parcel model allows to estimate updraft velocity for a given dry APSD functional shape and hygroscopicity.

## 5. ACKNOWLEDGEMENTS

This work was supported by Polish Ministry of Higher Education and Science with the statutory funds for research (2011/12) Faculty of Physics of University of Warsaw, (Institutes of Experimental Physics and of Geophysics) as well as of Institute of Applied Optics.

## 6. REFERENCES

[1]. Twomey S. and H. B. Howell. 1965. “The Relative Merit of White and Monochromatic Light for the Determination of Visibility by Backscattering Measurements.” *Applied Optics* 4: 501-506.

[2]. Khvorostyanov, V. I. and J. A. Curry. 1999. “A Simple Analytical Model of Aerosol Properties with Account for Hygroscopic Growth 1. Equilibrium Size Spectra and Cloud Condensation Nuclei Activity Spectra.” *Journal of Geophysical Research D: Atmospheres* 104 (D2): 2175-2184.

[3]. Celani, A., A. Mazzino, and M. Tizzi. 2008. “The Equivalent Size of Cloud Condensation Nuclei.” *New Journal of Physics* 10: 16.

[4]. Colón-Robles, M., R. M. Rauber, and J. B. Jensen. 2006. “Influence of Low-Level Wind Speed on Droplet Spectra Near Cloud Base in Trade Wind Cumulus.” *Geophysical Research Letters* 33 (20): L20814.

[5]. McFiggans, G., P. Artaxo, U. Baltensperger, H. Coe, M. C. Facchini, G. Feingold, S. Fuzzi, et al. 2006. “The Effect of Physical and Chemical Aerosol Properties on Warm Cloud Droplet Activation.” *Atmospheric Chemistry and Physics* 6 (9): 2593-2649.

[6]. Jagodnicka, A. K., T. Stacewicz, G. Karasiński, M. Posyniak, and S. P. Malinowski. 2009. “Particle Size Distribution Retrieval from Multiwavelength Lidar Signals for Droplet Aerosol.” *Applied Optics* 48 (4): B8-B16.

[7]. Bohren, C. F. and D.R Huffman. 1999. “Absorption and Scattering of Light by Small Particles.” *John Wiley & Sons, New York*.

[8]. Jagodnicka, A. K., T. Stacewicz, M. Posyniak, and S. P. Malinowski. 2009. “Aerosol Investigation with Multiwavelength Lidar.” *Proceedings of SPIE* 7479: 747903.

[9]. Apituley, A., A. Van Lammeren, and H. Russchenberg. 2000. “High Time Resolution Cloud Measurements with Lidar during CLARA.” *Physics and Chemistry of the Earth, Part B: Hydrology, Oceans and Atmosphere* 25 (2): 107-113.

[10]. Boers, R., H. Russchenberg, J. Erkelens, V. Venema, A. Van Lammeren, A. Apituley, and S. Jongen. 2000. “Ground-Based Remote Sensing of Stratocumulus Properties during CLARA, 1996.” *Journal of Applied Meteorology* 39 (2): 169-181.

[11]. Arabas, S., and H. Pawlowska. 2011. “Adaptive method of lines for multi-component aerosol condensational growth and CCN activation.” *Geoscientific Model Development* 4: 15-31.

[12]. Petters, M. D. and S. M Kreidenweis, 2007 “A single parameter representation of hygroscopic growth and cloud condensation nucleus activity”, *Atmos. Chem. Phys.*7, 1961-1971, doi:10.5194/acp-7-1961-2007,